J Mater Sci (2011) 46:2379–2383
DOI 10.1007/s10853-010-5085-0

Electrochemical fabrication and magnetic properties of Fe_7Co_3 alloy nanowire array

Jian Yang · Chunxiang Cui · Wei Yang · Bing Hu · Jibing Sun

Received: 22 September 2010 / Accepted: 12 November 2010 / Published online: 7 December 2010

Abstract A new type of magnetic material, Fe_7Co_3 nanowires, was successfully synthesized for the first time via a simple electrodeposition method. Highly uniform, self-ordered porous anodic aluminum oxide (AAO) membranes were prepared by the way of electrochemical. Fe_7Co_3 alloy nanowire arrays were fabricated in the porous alumina template in an aqueous solution of $FeCl_2$ and $CoCl_2$ by direct current electrodepositing. The microstructures of nanowires and AAO template were characterized by XRD, SEM, and TEM. The results show that a single Fe_7Co_3 nanowire is 40 nm in width and 2.5 μm in length with a preferred crystal face (110) during growing. The Fe_7Co_3 nanowire arrays have uniaxial magnetic anisotropy with easy magnetization direction along the nanowire axis due to the large shape anisotropy. It also shows that Fe_7Co_3 nanowire is a well-soft magnetic phase compared with Fe nanowires. It illustrates that Fe_7Co_3 possess higher saturation magnetization.

Introduction

A great amount of attention has been paid to the fabrication of magnetic nanowires recently for their potential utilization in ultra-high-density magnetic recording media [1–5]. A great deal of progress has been made in the synthesis of various nanostructures with controllable morphology and properties [6–10]. Currently, the nanowires are mainly fabricated on a template synthesis by porous alumina membranes [11]. Compared with other several different templates, the size of AAO holes can be readily controlled and the AAO template can be considered as a quicker and cheaper way to prepare highly perpendicular magnetic anisotropy nanowires [12–16].

It is well known that the $Fe_{1-x}Co_x$ alloy series have higher saturation magnetization [17]. Moreover, magnetic properties are not only influenced by the dimension and crystal properties but also depend on the physical structure [18, 19], so $Fe_{1-x}Co_x$ alloy series nanowires especially Fe_7Co_3 alloy nanowires with body centered cubic (bcc) structure have been a very interesting aspect of research because of large uniaxial magnetocrystalline anisotropy and higher saturation magnetization.

In this article, direct current electrodepositing method was adopted to fabricate Fe_7Co_3 nanowires which were prepared into porous anodic aluminum oxide (AAO) template. Their structural characteristics, chemical composition, and magnetic properties were studied in this article.

Experiment

Anodic aluminum oxide template was prepared by two-step methods, high purity (99.999%) Al sheets were anodized at 40 V and 283 K in 0.3 M oxalic acid solution. The first step was carried out for 4 h, and the second step was carried out for 8 h. The saturated $CuCl_2$ solution was used for removing the remaining Al substrate, and the 5 wt% H_3PO_4 solution was used for removing the barrier layer at 333 K for 40 min, then the nanopores with a diameter of 40 nm were formed. A thin Au layer was sprayed onto undersurface of the continuous holes film, and in this case, Au layer serves as the cathode during direct current electrodeposition. Fe_7Co_3 nanowire arrays were fabricated out by the nucleation and growth of Fe_7Co_3

J. Yang · C. Cui (✉) · W. Yang · B. Hu · J. Sun
School of Materials Science & Engineering, Hebei University of Technology, Tianjin 300130, China
e-mail: hutcui@hebut.edu.cn

embryos in the holes on the AAO templates using a direct current electrochemical deposition method. Here, the electrolyte consists of 0.35 M $FeCl_2$, 0.15 M $CoCl_2$, 2 g/L H_3BO_3, and 3 g/L ascorbic acid at a pH value of 2.4. Deposition was carried out at room temperature with a DC voltage of 2 V, using graphite as counter electrode. Fe nanowires were fabricated by the similar way besides the composition of the electrolyte is different (the electrolyte consists 0.35 M $FeCl_2$, 2 g/L H_3BO_3, and 3 g/L ascorbic acid at a pH value of 2.5). The solution was continuously agitated by a magnetic stirrer during the deposition. The Fe_7Co_3 and Fe nanowires were liberated from AAO template in the 10 wt% sodium hydroxide solution.

X-ray diffraction (XRD, Philips X'Pert MPD), scanning electron microscopy (SEM, Hitachi S-4800), and transmission electron microscopy (TEM, Philips Tecnai F20) were used to study the morphological feature, microstructure, and size of the AAO template and Fe_7Co_3 nanowires. The crystal structure of Fe_7Co_3 nanowires was investigated using a high-resolution transmission electron microscopy (HRTEM, Philips Tecnai F20) and selected area electron diffraction (SAED, Philips Tecnai F20), and average contents of Fe_7Co_3 nanowires were determined by field emission transmission electron microscope and energy dispersive X-ray spectrometer (FE-TEM/EDX, Philips Tecnai F20), and the magnetic properties of the samples were analyzed by vibrating sample magnetometer (VSM, Lake Shore Model-7407).

Results and discussion

The XRD pattern of as-deposited Fe_7Co_3 nanowire is shown in Fig. 1. It can be seen that X-ray diffraction measurements show three diffraction peaks: an especially strong peak occurring at 44.76°, a weaker peak at 82.45°, and the weakest peak at 65.12°. The XRD pattern is in agreement with the data of bulk or thin film of Fe_7Co_3 diffraction line standard (JCPDS Card Number 48-1618). These peaks show the deposition of Fe_7Co_3 nanowires with a preferred growth direction [110] along the crystallographic axis. The chemical reactions during the deposition of Fe_7Co_3 nanowires can be understood as follows:

$$\text{Oxidation} \quad OH^- - e^- \rightarrow 2H_2O + O_2 \uparrow$$

$$\text{Reduction} \quad 7Fe^{2+} + 3Co^{2+} + 20e^- \rightarrow Fe_3Co_7$$

$$2H^+ + 2e^- \rightarrow H_2 \uparrow$$

Fe_7Co_3 deposition could occur in the pores of the AAO template with the assistance of DC voltage, according to the formulations.

The SEM images in Fig. 2 show the top-view and the lateral-view of a porous alumina template which is used in this study. It is indicated in Fig. 2a that the average diameter of pores is about 40 nm and the length of nanoholes is about a few tens of micrometers. It is proved by the experiment that the diameter of nanoholes can be controlled by varying the anodized time.

Figure 3 is the schematic diagram to show the growth process of the Fe_7Co_3 nanowires during the deposition. There are three kinds of atomic arrangements of a single nanowire in the diagram which are in agreement with the XRD pattern. This diagram is only a simple show of three kinds of atomic stackings along with the crystal directions [110], [200], and [211], but not reveal the preferred growth direction [110] during the deposition.

Figure 4a shows typically the TEM images of as-grown Fe_7Co_3 nanowires liberated from template. The diameter of a single nanowire is 40 nm which is equal to the average diameter of pores in template and the length of nanowires is 2.5 μm. The aspect ratio (length to diameter) is 62.5, as expected they are looked continuous along all the length. There are some branches adhering the nanowires that can be seen in Fig. 4a, which is the remnant of alumina template cannot be removed. It is clearly indicated by Fig. 4b that the Fe_7Co_3 nanowires are polycrystalline structures which are further to be illustrated in Fig. 4c. And Fig. 4c also shows lattice diffraction contrast stripes image by the HRTEM image in which the interplanar distances are measured to be about 0.200, 0.140, and 0.113 nm which are in agreement with the (110), (200), and (211) crystalline planes of the Fe_7Co_3. Figure 4d shows a select area electron diffraction (SAED) pattern of the single nanowire. There are three strong and discontinuous rings with scattered spotty reflections, and the three rings are all indexed to (110), (200), and (211) reflections of bcc Fe_7Co_3 phase, illustrating that Fe_7Co_3 alloy nanowires are polycrystalline which is in accordance with the results of XRD, which proved that the deposited product are Fe_7Co_3 nanowires.

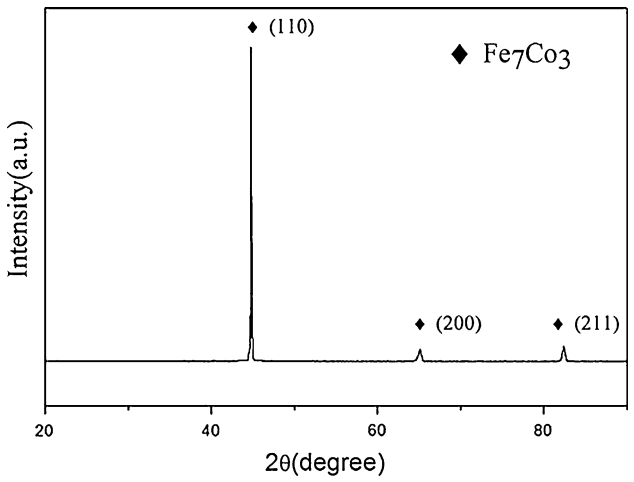

Fig. 1 X-ray diffraction pattern of Fe_7Co_3 nanowires embedded inside porous of the AAO template

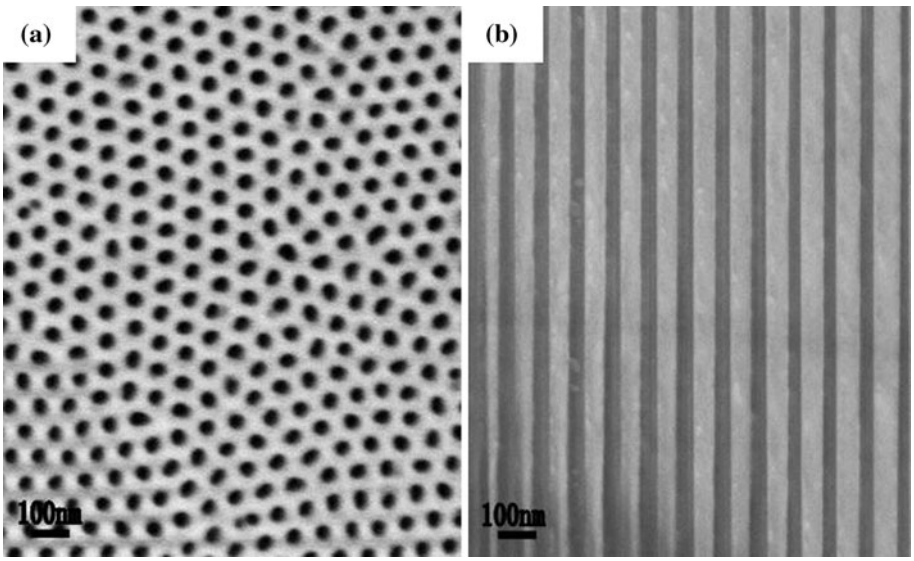

Fig. 2 SEM images of **a** top-view of AAO template and **b** lateral-view of AAO template

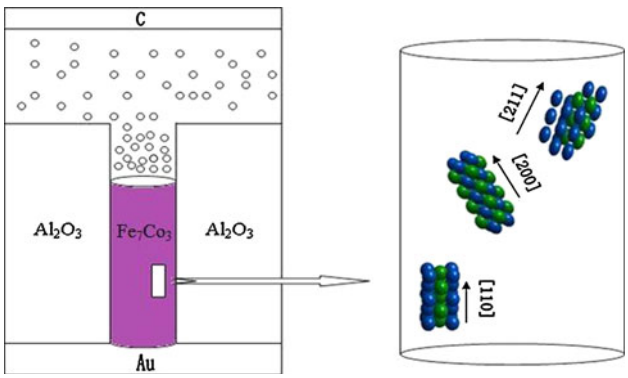

Fig. 3 The schematic diagram of growth process of the Fe_7Co_3 nanowire

To further verify the composition of as-prepared nanowires, the EDS test was recorded. As shown in Fig. 5 and Table 1, the atomic ratio of Fe and Co element is about 68.92/31.08 which can further demonstrates that the stoichiometric formula of deposited product is Fe_7Co_3.

The magnetic properties of Fe_7Co_3 nanowires arrays were studied by VSM with an external field of 5 KOe at room temperature. The M/MS-H loops of the as-prepared Fe_7Co_3 nanowires with external magnetic field parallel and perpendicular to the nanowires are displayed in Fig. 6. Obviously, the sample has an easy magnetic axis parallel to the axis of the nanowires. This indicates that the shape anisotropy is higher than magnetocrystalline anisotropy. It also shows that Fe_7Co_3 nanowires have typical soft magnetic behavior.

The magnetization in external magnetic field of ferromagnetic material is mainly influenced by atomic magnetic momentstructure. 4s electrons of outermost electronic shell orbit of 3d transition metals such as Fe and Co easily get rid of bound of atomic nucleus and become free electrons, therefore, the 3d orbit becomes the outermost orbit. As a consequence, it is very easily influenced by the vicinity metallic ions (positive) and become the adjacency orbit. Thus, magnetism arising from 3d unpaired electron orbit momentum can be ignored. To 3d transition metals, their atomic magnetic moment is mostly depended on their electron spin magnetic moment.

$$\left.\begin{aligned} &M_s(T) = -\mu_0 e/m_e \times \omega_e = -2M_B \eta s \quad (s = +1/2, -1/2) \\ &M_B = \mu_0 e/2m_e \\ &\eta = h/2\pi \end{aligned}\right\} \tag{1}$$

where μ_0 is the permeability of vacuum, e electron charge, m_e electron mass, ω_e spin angular momentum, M_B Bohr magneton, and h Planck constant.

According to the Slater-Pauling curve, Fe_7Co_3 in $Fe_{1-x}Co_x$ alloy series possesses the maximum $M_S(T)$ of about 2.5 M_B (Bohr magneton). Therefore, according to formula (1), Fe_7Co_3 should possess the highest saturation magnetization in $Fe_{1-x}Co_x$ alloy series [20, 21] and should be an excellent type of soft magnetic phase.

Permeability μ is the most important parameter that is used for characterizing the properties of soft magnetic phase.

$$\mu = \mu_0 + \mu_0 \triangle M/\triangle H \tag{2}$$

According to formula (2), the better soft magnetic phases should possess the higher permeability. Therefore, Fe_7Co_3 nanowires should possess higher permeability.

It is well known that Fe is a very excellent type of soft magnetic phase. In order to illustrate the soft magnetic properties of Fe_7Co_3 nanowires, Fe nanowires are

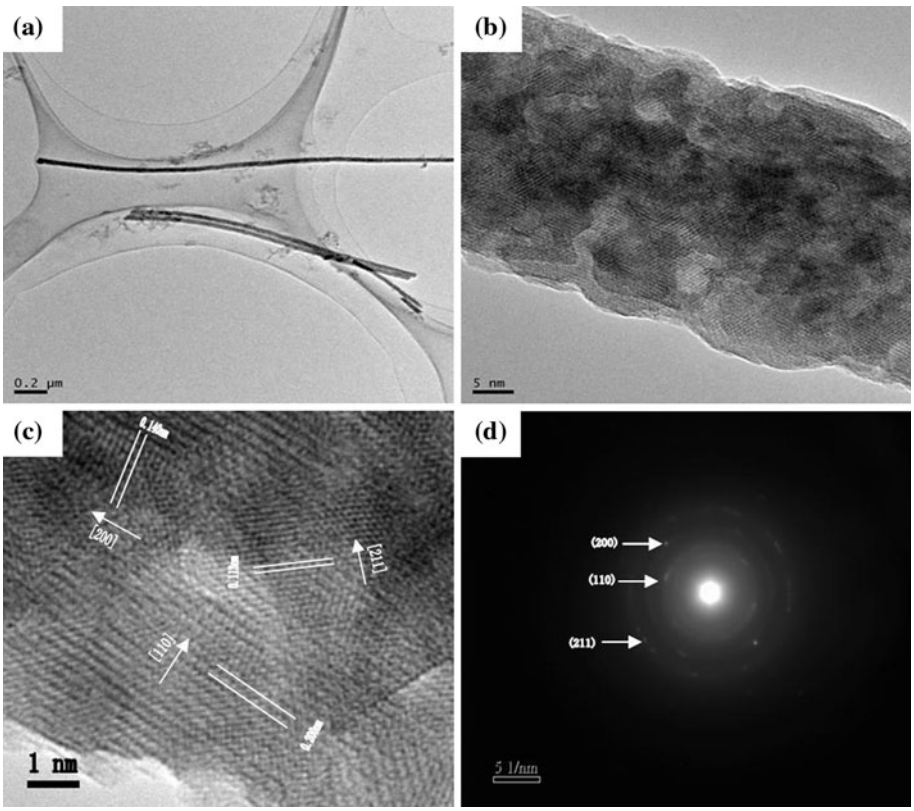

Fig. 4 Microstructures of as-deposited Fe_7Co_3 nanowire arrays. **a** TEM image of as-deposited Fe_7Co_3 nanowire arrays. **b** TEM image of a single Fe_7Co_3 nanowire with 40 nm in diameter. **c** The corresponding HRTEM image. **d** SAED pattern of a single nanowire

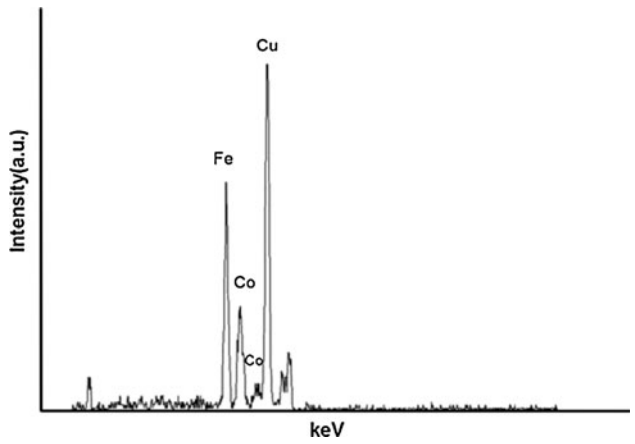

Fig. 5 Representative energy dispersive X-ray (EDX) spectra of Fe_7Co_3 alloy nanowires

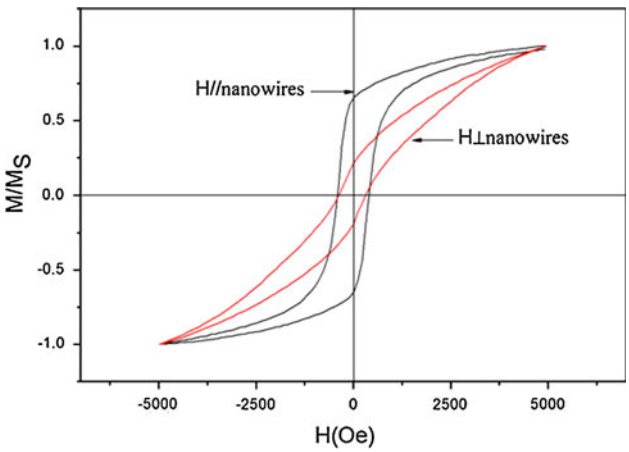

Fig. 6 Hysteresis loop of Fe_7Co_3 alloy nanowires at room temperature with an external field parallel and perpendicular to the axis of the nanowires

Table 1 Composition and atomic ratio of Fe_7Co_3 alloy nanowires

Element	Weight percentage	Atomic percentage
Fe K	67.76	68.92
Co K	32.24	31.08

used as comparison. Figure 7a shows the hysteresis loops of the Fe_7Co_3 and Fe nanowires at room temperature with an external field being parallel to the axis of the nanowires. It can be clearly seen that the Fe_7Co_3 nanowires possess higher saturation magnetization, while Fe_7Co_3 and Fe nanowires have the utterly close and low coercivity. The initial magnetic curves of Fe_7Co_3 nanowires and Fe nanowires are shown in Fig. 7b in which the permeability of Fe_7Co_3 nanowires is much higher than Fe nanowires. The result of Fig. 7 shows that Fe_7Co_3 nanowires is an excellent type of soft magnetic phase.

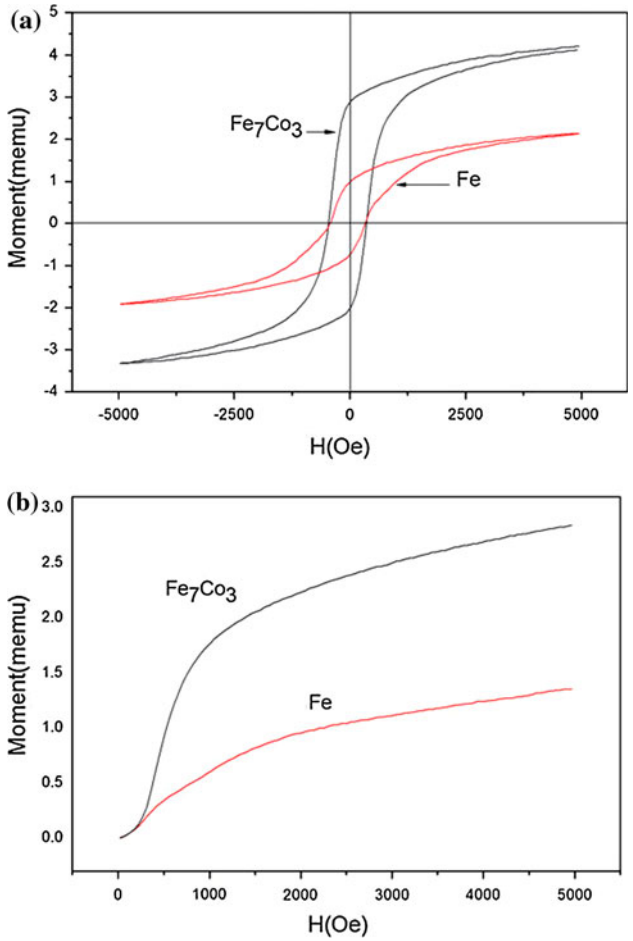

Fig. 7 Magnetic properties of Fe_7Co_3 alloy and Fe nanowires. **a** Hysteresis loop of Fe_7Co_3 alloy and Fe nanowires. **b** The initial magnetic curve of Fe_7Co_3 alloy and Fe nanowires

Conclusions

In conclusion, a new kind of Fe_7Co_3 nanowires arrays has been successfully synthesized for the first time via a simple electrodepositing method in this article. The result of XRD and HRTEM shows that the nanowires have a bcc polycrystalline. The hysteresis loop of the array demonstrates strong magnetic anisotropy with the easily magnetized direction being parallel to the nanowires axis. Fe_7Co_3 nanowire has the highest saturation magnetization in $Fe_{1-x}Co_x$ alloy series and it is one of the materials with high saturation magnetization and low coercivity which illustrates that Fe_7Co_3 nanowires can be used as an excellent soft magnetic phase in further application such as ultra-high-density magnetic recording media.

Acknowledgements This work is supported by Natural Science Foundation of Hebei Province with No. E2010000125. And this work is partly supported by Tianjin Natural Science Foundation (09JCZDJC22800).

References

1. Lin SC, Chen SY, Chen YT, Cheng SY (2008) J Alloys Compd 449:232
2. Yin AJ, Li J, Jian W, Bennett AJ, Xu JM (2001) Appl Phys Lett 79:1039
3. Shima M, Hwang M, Ross CA (2003) J Appl Phys 93:3440
4. Ji GB, Chen W, Tang Sl, Gu BX, Li Z, Du YW (2004) Solid State Commun 130:541
5. Yuan XY, Wu GS, Xie T, Lin Y, Meng GW, Zhang LD (2004) Solid State Commun 130:429
6. Schmitt AL, Higgins JM, Jin S (2008) Nano Lett 8:810
7. Zhang D, Liu Z, Han S, Li C, Lei B, Stewart MP et al (2004) Nano Lett 4:2151
8. Schwedhelm R, Kipp L, Dallmeyer A, Skibowski M (1998) Phys Rev B 58:13176
9. Saab AP, Laub M, Srdanov VI, Stucky GD (1998) Adv Mater 10:462
10. Luo Z, Fang Y, Zhou X, Yao J (2008) Mater Chem Phys 107:91
11. Chu SZ, Inoue S, Wada K, Kurashima K (2005) Electrochim Acta 51:820
12. Pruneanu S, Olenic L, Al-Said SAF et al (2010) J Mater Sci 45:3151. doi:10.1007/s10853-010-4320-z
13. Yang W, Cui CX, Sun JB et al (2010) J Mater Sci 45:1523. doi:10.1007/s10853-009-4116-1
14. Zhu ZF, Sun HJ, Liu H et al (2010) J Mater Sci 45:46. doi:10.1007/s10853-009-3886-9
15. Qin L, Zhang J, Shen TH et al (2010) J Mater Sci 45:1130. doi:10.1007/s10853-009-4058-7
16. Tien LC, Pearton SJ, Norton DP et al (2008) J Mater Sci 43:6925. doi:10.1007/s10853-008-2988-0
17. Kuhrt C, Schultz L (1992) J Appl Phys 71:1896
18. Xu CL, Qin DH, Li H, Guo Y, Xu T, Li HL (2004) Mater Lett 58:3976
19. Shao I, Chen MW, Cammarata RC, Searsom PC, Prokes SM (2007) J Electrochem Soc 154:572
20. Wang Z, Liu X, Lv M, Meng J (2010) Mater Lett 64:1219
21. Tian MB (2001) Magnetic Materials. Tsinghua, Beijing (in Chinese)